

Threshold ionization mass spectrometry in the presence of excited silane radicals

This article has been downloaded from IOPscience. Please scroll down to see the full text article.

2009 J. Phys. D: Appl. Phys. 42 072003

(<http://iopscience.iop.org/0022-3727/42/7/072003>)

View [the table of contents for this issue](#), or go to the [journal homepage](#) for more

Download details:

IP Address: 38.107.179.212

The article was downloaded on 21/02/2012 at 14:24

Please note that [terms and conditions apply](#).

FAST TRACK COMMUNICATION

Threshold ionization mass spectrometry in the presence of excited silane radicals

T Moiseev¹, D Chrastina¹, G Isella¹ and C Cavallotti²¹ Politecnico di Milano, Reg. di Como, L-NESS, Via Anzani 42, Como, 22100 (CO), Italy² Politecnico di Milano, Dipt. Chimica, Materiali e Ing. Chimica, 'G. Natta', Via Mancinelli 7, Milano, 20131 (MI), ItalyE-mail: tamara.moiseev@como.polimi.it

Received 28 November 2008, in final form 19 January 2009

Published 13 March 2009

Online at stacks.iop.org/JPhysD/42/072003

Abstract

The presence of excited radicals in plasma-assisted chemical vapour deposition silane processes leads to overestimation of radical densities in threshold ionization mass spectrometry analysis. A method to discriminate the signal due to excited radicals is proposed and applied to estimate the relative density trends of the ground-state silane radicals (SiH_x , $x < 4$) with hydrogen input flow rates (0–50 sccm) in an argon–silane–hydrogen plasma at total pressures of 0.01–0.04 mbar used for the deposition of nano-crystalline silicon (nc-Si) layers for photovoltaic applications. The $\text{SiH}_x/\text{SiH}_4$ density trends with hydrogen input show a turning point where SiH becomes dominant, in the process region where nc-Si layers were previously obtained.

(Some figures in this article are in colour only in the electronic version)

1. Introduction

Threshold ionization mass spectrometry (TIMS) can be an important tool for optimization of plasma-assisted chemical vapour deposition (PECVD) processes in the transition zone from amorphous to crystalline layers for nano-crystalline silicon (nc-Si) deposition in photovoltaic applications.

PECVD processes generate silane radicals on electronically or ro-vibrationally excited states, such species having much larger ionization cross-sections with lower thresholds [1]. While the densities of excited radicals are generally low, their increased ionization cross-sections lead to overestimations in TIMS analysis. An improved TIMS method is proposed in order to discriminate the excited radical signal from the ground-state one when the analysis indicates the presence of excited silane radicals.

This study observes TIMS relative densities of ground-state silane radicals and their evolution with hydrogen input in the low-energy plasma-enhanced chemical vapour deposition (LEPECVD) [2, 3] plasma used for the deposition of nc-Si layers at low temperature (200–250 °C) and fast growth rates

(1.3–3.5 nm s⁻¹) required in solar cell applications. The improved analysis allows the evaluation of silane radicals (SiH_x ; $x < 4$) over an extended range of hydrogen flow rates, revealing that their density trends in the process region for nc-Si deposition [4] have a turning point where the most abundant radical is SiH instead of SiH_3 .

2. Experimental set-up

The LEPECVD process is based on a low energy hot filament dc arc discharge (50 A) at 20–30 V in argon–silane–hydrogen at total pressures of 0.01–0.04 mbar. The argon gas inlet and the hot filament are situated at the base of the reactor. The filament heated by 130 A ac emits electrons confined by an axial magnetic field ($B \leq 1.2$ mT) generated by coils surrounding the reactor and reach the wafer region where silane and hydrogen gas are added by a ring-shaped inlet. The wafer is biased at floating potential (–12 V to –14 V) and its temperature is regulated at 200 °C. Reactor base pressures are in the UHV range (10⁻⁹ mbar).

A HIDEN analytical EQP300 quadrupole mass spectrometer has been used for TIMS analysis. The electrostatic quadrupole plasma (EQP) probe operated at floating potential is positioned at the wafer level. TIMS data have been acquired at 3 cm from the wafer edge. A pressure below 8×10^{-7} mbar is maintained inside the spectrometer by a C&Rlikon TMP361 turbo pump. The measurements were performed using a $300 \mu\text{m}$ sampling orifice, time-integration (dwell time) 3000 ms, RGA filament current of $80 \mu\text{A}$ and scanning electron energy in the range from 7 to 20 eV. The $80 \mu\text{A}$ filament emission current has been chosen below the values leading to the formation of space-charge [5] inside the ionizer (which here occurs for emission currents starting at $100 \mu\text{A}$). The electron energy scale calibration has been performed by the linear extrapolation method using a pure Ar discharge. An off-set of about +0.5 eV has been observed and the energy scale has been corrected accordingly.

3. The TIMS method

TIMS analysis of radical densities is based on selective ionization of each radical using electron energies between the ionization potential (IP) of the given radical (threshold E_1) and the threshold E_{DI} for dissociative ionization (DI) towards the same radical starting from silane. The relative density of species can be determined from the formula [6, 7]:

$$\frac{n(\text{A})}{n(\text{AB})} = C \frac{\sigma_{\text{DI}}(E_2 > E_{\text{DI}})}{I(E_2 > E_{\text{DI}})} \times \frac{1}{E_1' - E_1''} \int_{E_1''}^{E_1'} \frac{\Delta I(\text{A}^+, E)}{\sigma_1(E)} dE, \quad (1)$$

where I , ΔI are the number of counts at each energy (above the DI threshold and, respectively, between the I and DI thresholds) σ_1 and σ_{DI} the cross-sections for ionization of the given neutral radical (A) and DI of parent molecule (AB) towards A. The energy interval for integration is chosen so that $E_1 < E_1' - E_1'' < E_{\text{DI}}$. The net radical signal from the plasma is

$$\Delta I(\text{A}^+) = (I(\text{A}^+)_{\text{ON}} - I(\text{A}^+)_{\text{ions}}) - I(\text{A}^+)_{\text{OFF}} \cdot \frac{n(\text{AB})_{\text{ON}}}{n(\text{AB})_{\text{OFF}}}, \quad (2)$$

where I_{ON} and I_{OFF} are the signals during plasma on and off and $I(\text{A}^+)_{\text{ions}}$ is the ion background signal given by ions generated by the discharge (during plasma on).

The ion current has been measured at both a zero emission filament current ($I_f = 0 \mu\text{A}$) and at $I_f = 1 \mu\text{A}$ and subtracted according to (2). The measurements at $I_f = 1 \mu\text{A}$ serve as a reference level in this work as they provide an active control over the filament temperature (and emission) during ion background measurements and there are negligible differences from values with $I_f = 0 \mu\text{A}$ in the energy region below the DI thresholds. No other background signal was observed for discharge off, filament off ($I_f = 0 \mu\text{A}$) while any noise signal during plasma on and $I_f = 0 \mu\text{A}$ (or $I_f = 1 \mu\text{A}$) is included in the measured ion background.

The coefficient C , which describes the residence time of silane inside the spectrometer [8], was estimated for a pumping

speed $S = 300 \pm 30 \text{ s}^{-1}$, 300 K gas temperature and a distance $l = 4.5 \text{ cm}$ between the ionizer and the sampling orifice, at $C = 10 \pm 2$. Lower pumping speeds, higher gas temperatures or kinetic energies of the radicals will lead to higher C values, especially for lower mass radicals. To avoid overestimations at lower mass radicals we have considered $C = 10$ throughout the calculations.

The cross-sections proposed as analytical fit functions by Janev and Reiter [9] have been used as they provide partial cross-sections with corrections for the energy dependent branching ratios between reaction thresholds and errors within 20% accuracy of the experimental data.

4. Improved TIMS analysis

The main non-systematic errors of the TIMS method come from the choice of the $E_1' - E_1''$ range limits for integration. The upper limit can be chosen at the DI threshold (as the DI cross-section at the threshold is too low to give significant counts) while the choice of the lower limit is related to background signal discrimination.

Counting ions produced inside the ionizer at electron energies close to the IP of the radical, relating low counting rates to very low cross-sections, leads to large errors in the estimation of radical densities. These can be avoided by choosing E_1' at a higher energy where ionization cross-sections have larger values. The signal lost by shortening the energy interval corresponds to regions with low ionization cross-sections leading to a low and random signal that is not a relevant quantity.

A significant source of errors is the presence of excited radicals (molecular species on vibrational/rotational or electronically excited levels) generated mainly through electron impact excitation or ion-electron recombination, some leading to highly excited (Rydberg states) long-lived molecules [10, 11]. Although the presence of excited molecules in process plasmas has been observed and their influence on the evolution of process parameters is expected to be significant, there is a lack of data concerning their cross-sections [12] and recent studies show that such species have much larger ionization cross-sections with thresholds shifted towards lower energies.

Typical electron energy scans are shown in figures 1 and 2, where the signals for plasma on (ON, $I_f = 1 \mu\text{A}$) plasma off (OFF) corrected for silane depletion (OFF corrected) and ion background (ON, $I_f = 1 \mu\text{A}$) are indicated on each graph. The ion background signal is shown for a filament current of $I_f = 1 \mu\text{A}$ instead of $I_f = 0$ to emphasize the excess signal between the total radical signal for plasma on and the measured ion background. A strong signal above the ion background but below the IP thresholds (IP = 8.01 eV for SiH_3 and IP = 7.91 eV for SiH) [9] can be observed, this situation being common for all radicals and gas mixtures. Such a signal can be ascribed to excited radicals that have high ionization cross-sections with thresholds at much lower energies. Integrating the signal between the ion background (ON, $I_f = 1 \mu\text{A}$) and the one for 'plasma on' (ON $I_f = 80 \mu\text{A}$), as required by

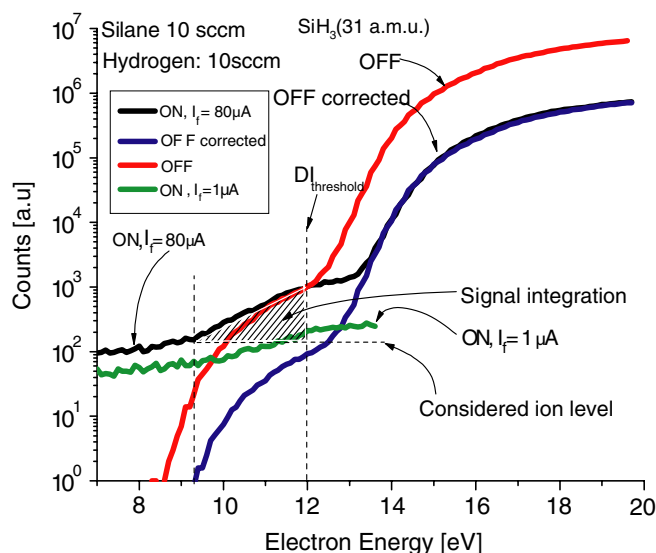


Figure 1. TIMS data for SiH_3 radical at 10 sccm silane and 10 sccm hydrogen input.

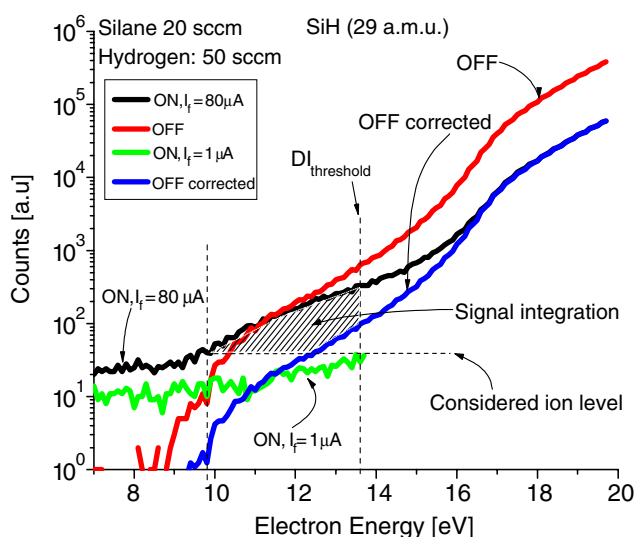


Figure 2. TIMS data for SiH radical at 20 sccm silane and 50 sccm hydrogen input.

formula (2), leads to radical density overestimation of orders of magnitude, exceeding total silane density.

The semi-log signal for plasma on (figures 1 and 2) shows a clear change in slope situated 1–1.5 eV above the IP thresholds indicating the occurrence (dominance) of another process (the ionization of the ground-state radicals) superimposed on the signal given by ionization of excited radicals that reaches saturation (the constant signal level below the IP threshold). This observation provides a means to set the lower integration limit for the estimation of ground-state radicals.

In this work the influence of excited species on the overall count is minimized by considering the ion background level as the count level at the above change in the signal slope, thus including the excited radical signal in the ion background. This is justified as cross-sections of excited radicals are much larger than those of ground-state radicals and the number of counts that can be ascribed to excited species corresponds to a low density of such species.

The considered interval for signal integration is indicated by the hashed area having as limits the energy corresponding to the first change in slope (lower limit), the DI threshold towards the given radical from SiH_4 (upper limit) and as ion background the count level at the slope change (indicated as ‘considered ion level’). The lower limit of integration changes with hydrogen input (within 0.5–1.5 eV above IP threshold) depending on the density ratio of excited to ground-state species and had to be assessed for each case.

Starting the integration at higher energies is advantageous in lowering the error levels from both the discussed points of view: the signal is counted at energies well above the IP threshold where ionization cross-sections are higher and a steady increasing signal above the one from the excited radicals allows for discrimination.

Detection efficiency is affected by the surface reactivity of silane radicals. Corrections involving sticking coefficients lead to an increase in the estimated relative densities mainly for SiH and Si radicals (with sticking coefficients close to 100%). Such corrections have not been applied here explicitly. Choosing silane as a reference gas and calculating its density from the count levels of each radical includes corrections for residence times and sticking coefficients which should be similar when monitoring the same radical during either discharge on or off as required by the method.

5. Results and discussion

TIMS measurements have been performed for SiH_x ($x < 4$) at two silane flow rates Φ_{SiH_4} (10 and 20 sccm) and a range of hydrogen flow rates Φ_{H_2} (0–50 sccm) leading to a silane dilution in hydrogen $d = \Phi_{\text{SiH}_4} / (\Phi_{\text{SiH}_4} + \Phi_{\text{H}_2})$ in the range from 1 to 0.17. At each silane–hydrogen gas mixture TIMS analysis was performed for the silane radicals considering only the main DI reactions starting from SiH_4 , using the reduced electron energy intervals for each radical as shown previously to improve the error level for measurements in the presence of excited radicals. The obtained relative density trends of SiH_x ($x < 4$) radicals with the addition of hydrogen are shown in figures 3 and 4 for silane flow rates of 10 and 20 sccm. The error bars correspond to the relative difference between radical densities reported to the silane level (during off time) calculated from the DI signal at 17 eV and at 20 eV. If the σ_{DI} energy dependence is accurate, the deviation between radical densities calculated with readings at two energy values estimates the error due to measurement.

The observed density of Si neutral radical is very small, below 0.005% for all situations, with large errors due to low counting rates as a result of its fast recombination rate in the gas phase and its high reactivity to surfaces, significant loss being expected as deposition inside the spectrometer before reaching the ionizer.

At low hydrogen input (0–20 sccm) increasing density trends of the SiH_x ($1 < x < 4$) radicals can be observed for both 20 sccm and 10 sccm silane input. These can be ascribed to a combined effect of electron impact dissociations and hydrogen–silane gas-phase reactions under the increasing density of free hydrogen atoms with the addition of hydrogen.

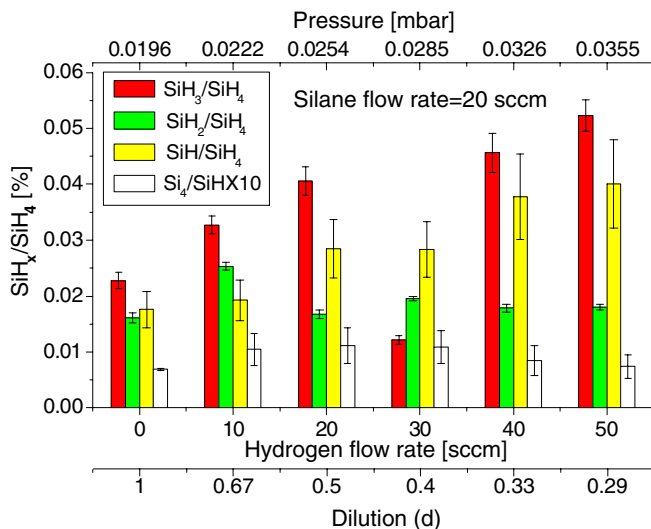


Figure 3. Evolution of SiH_x ($x < 4$) relative densities with hydrogen input for 20 sccm silane input.

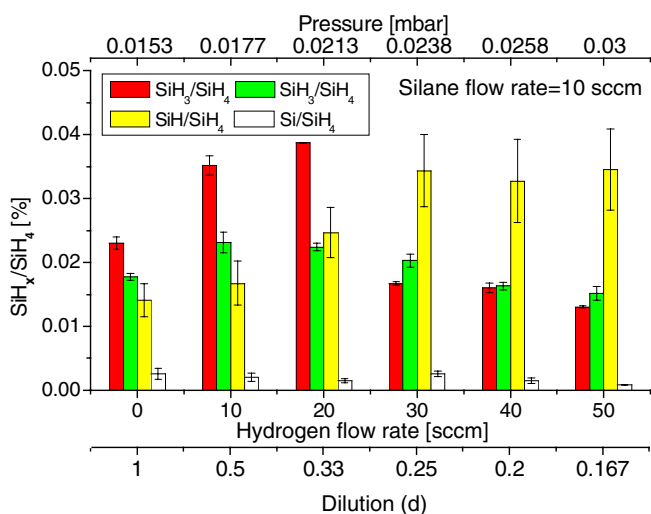


Figure 4. Evolution of SiH_x ($x < 4$) relative densities with hydrogen input for 10 sccm silane input.

Above 20 sccm hydrogen input the two charts show significant differences in trends, the SiH radical becoming the dominant radical for the 10 sccm silane flow rate (figure 4).

While TIMS analysis reported by other authors often did not allow for direct estimations of SiH density, the presence of SiH in rf PECVD plasmas is known and used for OES monitoring of the $\mu\text{c-Si}$ deposition [13–16]. As observed by Perrin [17], the high OES signal obtained for SiH* makes this radical a non-negligible participant in the deposition process.

Previously reported [4] Raman crystallinity of nc-Si samples grown by LEPECVD show a strong increase in crystalline fraction with increase in silane dilution, a transition zone between low and high crystallinity being obtained for $\Phi_{\text{SiH}_4} = 10\text{--}12$ sccm at $d = 0.3\text{--}0.25$, corresponding to the observed (figure 4) turning point in radical relative densities, where SiH is dominant.

The formation of lower silane radicals (SiH, Si) can take place at low silane input (allowing for high silane depletion) due to either electron impact dissociation of the higher silane

radicals (SiH_3 , SiH_2) into lower ones (SiH, Si) or by H abstraction from SiH_x leading to SiH_{x-1} ($0 < x < 4$) at high hydrogen input. Therefore, the requirements for high silane depletion and high silane dilution observed in the optimization of micro-crystalline silicon ($\mu\text{c-Si}$) growth [18–21] are also met here, leading to the depletion of higher silane radicals towards the lower ones.

6. Conclusions

The improved TIMS method allows for the observation of the four mono-silane radicals (SiH_3 , SiH_2 , SiH and Si) and reveals the trends in their relative densities with the addition of hydrogen in argon–silane–hydrogen plasmas.

For the LEPECVD process, a turning point in SiH_x ($x < 4$) relative densities is obtained in the process region for nc-Si deposition, where the most abundant radical is no longer SiH_3 but the SiH radical, the latter maintaining the highest densities with further increase in hydrogen input.

This study shows that significant changes in plasma composition occur at high silane dilution in hydrogen, leading to increased generation of SiH which becomes the dominant radical, suggesting that SiH is a main precursor in the growth of nc-Si layers by LEPECVD and that the changes in plasma composition are the main factor leading to nc-Si growth.

Acknowledgments

This work has been funded by the European Commission, Nanophoto Project Contract no 013944. The authors are grateful to Professor Hans von Känel from ETH Zürich for providing new lab equipment for use on this project.

References

- [1] Cristophorou L G and Olthoff J K 2004 *Fundamental Electron Interactions with Plasma Processing Gases* (Berlin: Springer)
- [2] Kummer M, Rosenblad C, Dommann A, Hackbarth T, Höck G, Zeuner M, Müller E and von Känel H 2002 *Mater. Sci. Eng. B* **89** 288–95
- [3] Pizzini S *et al* 2006 *Mater. Sci. Eng. B* **134** 118
- [4] Le Donne A, Binetti S, Isella G, Pichaud B, Texier M, Acciarri M and Pizzini S 2008 *Appl. Surf. Sci.* **254** 2804–8
- [5] Agarwal, S, Quax G W W and van de Sanden M C M, Maroudas D and Aydil E S 2004 *J. Vac. Sci. Technol. A* **22.1** 71–81
- [6] Robertson R, Hills D, Chatam H and Gallagher A 1983 *Appl. Phys. Lett.* **43** 544–6
- [7] Kae-Nune P, Perrin J, Guillon J and Jolly J 1994 *Japan. J. Appl. Phys.* **33** 4303–7
- [8] Kae-Nune P, Perrin J, Guillon J and Jolly J 1995 *Plasma Sources Sci. Technol.* **4** 250–9
- [9] Janev R K and Reiter D 2003 *Contrib. Plasma Phys.* **43** 401–17
- [10] Stebbings R F and Dunning F B (ed) 1983 *Rydberg States of Atoms and Molecules* (Cambridge University Press: Cambridge)
- [11] Nagesha K and Pinnaduwa L A 1999 *Chem. Phys. Lett.* **312** 19–27
- [12] Cristophorou L G and Olthoff J K 2002 *Appl. Surf. Sci.* **192** 309–26

- [13] Amanatides E, Mataras D, Rapakoulias D, van den Donker M N and Rech B 2005 *Sol. Energy Mater. Sol. Cells* **87** 765–805
- [14] Howling A A, Strahm B, P. Colsters P, Sansonnens L and Hollenstein Ch 2007 *Plasma Sources Sci. Technol.* **16** 679–96
- [15] Wu Z, Sun J, Lei Q, Zhao Y, Geng X and Xi L 2006 *Physica E* **33** 125–9
- [16] Strahm B, Howling A A and Hollenstein Ch 2007 *Plasma Phys. Control. Fusion* **49** B411–8
- [17] Perrin J, Leroy O and Bordage M C 1996 *Contrib. Plasma Phys.* **36** 3–49
- [18] Strahm B, Howling A A, Sansonnens L and Hollenstein Ch 2007 *J. Vac. Sci. Technol. A* **25** 1198–202
- [19] Strahm B, Howling A A, Sansonnens L and Hollenstein Ch 2007 *Plasma Sources Sci. Technol.* **16** 80–9
- [20] Kondo M, Fukawa M, Guo M L and Matsuda A 2000 *J. Non-Cryst. Solids* **266–269** 84–9
- [21] Matsuda A 2004 *J. Non-Cryst. Solids* **338–340** 1–12